"This is the accepted manuscript of the following article: Gallo, P. (2018), Fracture Behavior of Nanoscale Notched Silicon Beams Investigated by the Theory of Critical Distances. Adv. Theory Simul. doi:10.1002/adts.201700006, *which has been published in final form at* https://doi.org/10.1002/adts.201700006. *This article may be used for non-commercial purposes in accordance with Wiley Terms and Conditions for Use of Self-Archived Versions."*

Fracture Behavior of Nanoscale Notched Silicon Beams Investigated by the Theory of Critical Distances

Pasquale Gallo, Yabin Yan, Takashi Sumigawa, and Takayuki Kitamura*

Dr. P. Gallo, Dr. Y. Yan, Prof. T. Sumigawa, Prof. T. Kitamura
Kyoto University, Department of Mechanical Engineering and Science
Kyoto-daigaku-Katsura, Nishikyo-Ku, Kyoto-Shi, 615-8540, Japan
E-mail: pasquale.gallo@aalto.fi

Keywords: nanoscale, single crystal silicon, theory of critical distances, fracture toughness, notches

This paper investigates the nanoscale fracture behavior of silicon using the Theory of Critical Distances (TCD) and demonstrates that TCD can correctly estimate the magnitude of the breakdown of continuum fracture mechanics. Moreover, it proposes the TCD as an alternative strategy for the determination of fracture toughness, K_{IC}, at the nanoscale. More specifically, in situ micromechanical testing of notched nano-cantilever beams has been carried out in a transmission electron microscope. The material characteristic length and fracture toughness are then evaluated. The average K_{IC} value obtained is 0.98 MPa·m$^{0.5}$, which is in agreement with that reported in the literature for macro-Si. The characteristic material length is in the range of 0.65-0.95 nm. It is found that within an atomistic interpretation of the fracture of silicon, these values are in agreement with the breakdown of continuum fracture mechanics.

1. Introduction

With the continuous miniaturization of electronic devices driven by the ever-increasing demand for high-density integration, the size of elements has been approaching several

nanometers. In some cases, the atom-by-atom structure has been considered.[1–3] Examples of such devices are micro- and nano-electromechanical systems (MEMS and NEMS), made of single-crystal silicon and employed as sensors and actuators. These new advances have brought problems of material behavior at the micro/nanometer scale into the domain of fracture mechanics, and a precise characterization of the mechanical properties of silicon is essential for the proper design of structural elements in micro- and nanodevices. Indeed, the small dimensions of MEMS and NEMS pose a tremendous challenge for experimental studies, which prevents the development of numerical and theoretical tools to design those small components.[4] While considerable effort has been devoted to determining Young's modulus and tensile strength of silicon and other materials,[5–9] fracture properties have sparked the interest of the scientific community only recently. Indeed, in recent years, several methods for determining the mechanical properties of nano- and micro-components have been developed, e.g., tensile tests, bending tests, indentation, and the thermal stress method. *In situ* observation of mechanical behavior has advanced as well.[10–13] Sumigawa et al.[10] published a review of a series of experimental studies at small scales. The authors concluded that the "stress," whose concept is based on continuum mechanics, is still applicable to the fracture phenomenon as the governing parameter while the size approaches the atomic scale. This valuable contribution suggests that the extension of well-known linear elastic fracture mechanics (LEFM) to very small scales is possible, provided that its breakdown is well defined. Among the attempts at extending certain LEFM concepts and methods to the nanoscale, the contribution by Gallo et al.,[14] who tried to extend the averaged Strain Energy Density[15,16] concept to the nanoscale, is worth mentioning. Other researchers have focused on the thermomechanical and fracture properties of single-crystal silicon at elevated temperatures, particularly the brittle-ductile temperature transition.[17,18] Recent studies have investigated the cracking behavior from a notch tip in Si films.[19–21] The measured fracture toughness was found to be dependent on the loading direction and independent of the specimen surface orientation. The K_{IC} obtained was different from the value of bulk silicon. Indeed, these results were affected by the finite radius of curvature at the crack tip, which did not permit the size dependence of nanoscale fracture toughness to be highlighted correctly. This example demonstrated that it could be challenging to fabricate a precracked specimen and a small radius may affect the final K_{IC} value. Recently, the fracture toughness of silicon has been determined in a nanoscale singular stress field by other researchers.[22] More specifically, the cracking behavior was investigated by using single-crystal silicon specimens with different precrack lengths. The singular stress field obtained was between 23 nm and 58

nm, and the geometry of the crack tip was accurately realized to avoid large curvatures. The fracture toughness obtained showed good agreement with the bulk K_{IC}, but as the authors underlined, the fabrication of a cracked component at such a small scale was very challenging. Moreover, they employed a large number of specimens to obtain a reliable estimation. Several attempts at measuring the fracture toughness of single-crystal silicon by avoiding the realization of the crack geometry have involved indentation methods.[23] The results, which were obtained through complex molecular dynamics simulations and by using a large number of samples, did not include any contribution from the plastic work. In summary, cracked specimens are difficult to obtain at the nanoscale, and a large number of samples is needed to obtain a reliable $K_{IC.}$ On the other hand, when alternative methods simplify the testing procedure, e.g., indentation methods,[23] very complex and time-consuming post-processing steps are required to determine the fracture toughness, and once again, a large number of samples is necessary.

Against this background, the present paper proposes the Theory of Critical Distances (TCD)[24] as an alternative strategy for the characterization of fracture behavior at the nanoscale. The main advantage of the TCD is that K_{IC} can be estimated accurately by testing samples containing notches of at least two different sharpnesses,[25] without any need for a cracked specimen or any other restriction on the geometry. This solution greatly simplifies the experimental procedures. It also gives insight into the breakdown of fracture mechanics at small scales by comparing the TCD material characteristic length with values reported in recent studies.[26,27] It is found that when an atomistic interpretation of fracture is provided, the critical distance obtained is in agreement with the lower applicable limit (dimensional bound) for fracture mechanics, i.e., 1.5-3 nm.[27] Thus, as long as continuum mechanics remains valid, the same atomic length scale governs the fracture of silicon in the case of notches, cracks and from the nano- to macroscale.

2. Results

2.1 Loading Experiments

Four specimens made of single-crystal Si were prepared by a focused ion beam (FIB) processing system. Details on the mechanical properties of Si, fabrication process and steps are reported in the Experimental Section and Supporting Information S1. The final geometry is verified *a posteriori* by re-analyzing the Scanning Electron Microscope (SEM) images.[28] TCD only requires a comparison of different sharpnesses without any specific restriction on the geometry, which offsets the difficulty of achieving a precise notch radius and shape. Four

nano-cantilevers were obtained with notch radii of 10.2, 6.3, 20.2 and 13.8 nm and opening angles 2α of 33°, 68°, 59° and 48° respectively. The final geometrical parameters are shown in **Figure 1** and listed in **Table 1**. These geometries result in the following stress concentration factors, K_{tn}: 4.3, 4.9, 2.9 and 3.7 for specimen numbers 1, 2, 3 and 4, respectively.

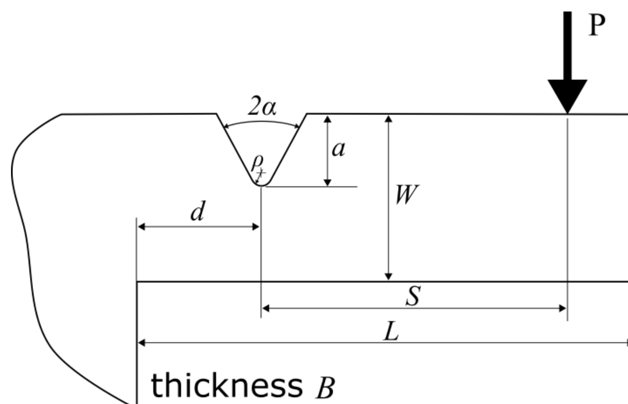

Figure 1. Schematics of the nano-cantilever and notch

Table 1. Geometrical parameters of the nano-cantilever beams and notches

Specimen	B [nm]	W [nm]	L [nm]	2α [deg]	ρ [nm]	a [nm]	d [nm]	S [nm]
1-side A	494	502	1307	33	10.2	155	217	837
1-side B	492	499	1307	37	3.4	54	229	825
2	454	456	1252	68	6.3	144	87	875
3	484	495	1201	59	20.2	179	119	651
4	529	544	1019	48	13.8	161	96	682

The notches are aligned along the $[1\bar{1}0]$ direction, while the beam is developed in the [100] direction (please see **Figure S1**, Supporting Information). This orientation is different from those reported in the few previous studies available which mainly focus on the cleavage plane Si(011) and the [100] direction.[22] Therefore, the experimental configuration proposed here allows the determination of any influence of orientation on fracture toughness by simple comparison. The notches show good symmetry on the two lateral surfaces and the average values are taken as the nominal value. Specimen number 1, on the other hand, has been fabricated with asymmetric notches to determine the sensitivity of the method to the precision of nano-beam fabrication. The results suggest that fracture occurs first on the side where the depth of the notch is higher (side 1-A in Table 1). Therefore, that geometry has been assumed as the nominal in subsequent analyses. **Figure 2** shows SEM images of the specimens and notches.

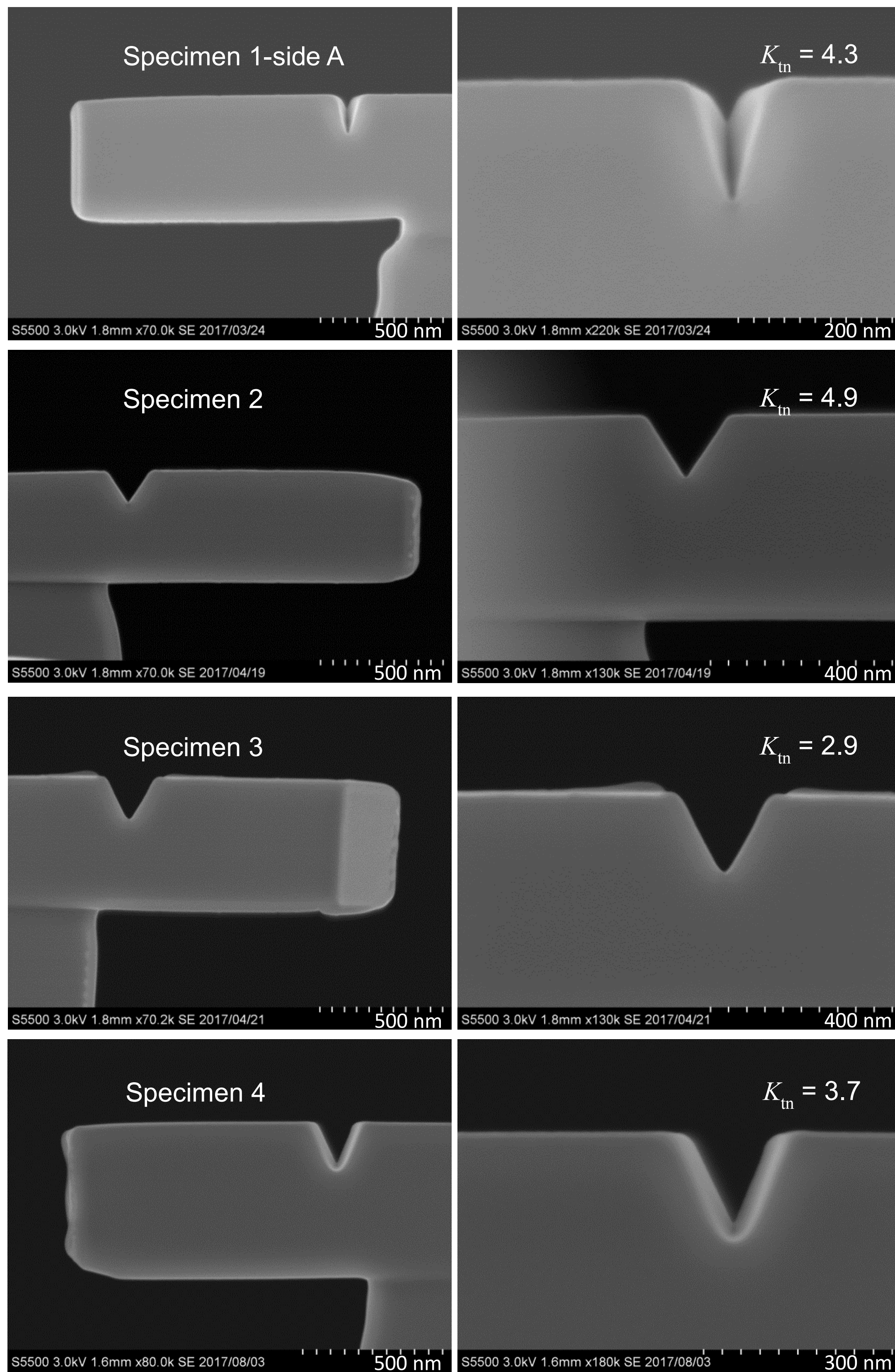

Figure 2. SEM images of specimens: nano-cantilever beam (left) and close-up of the notch (right).

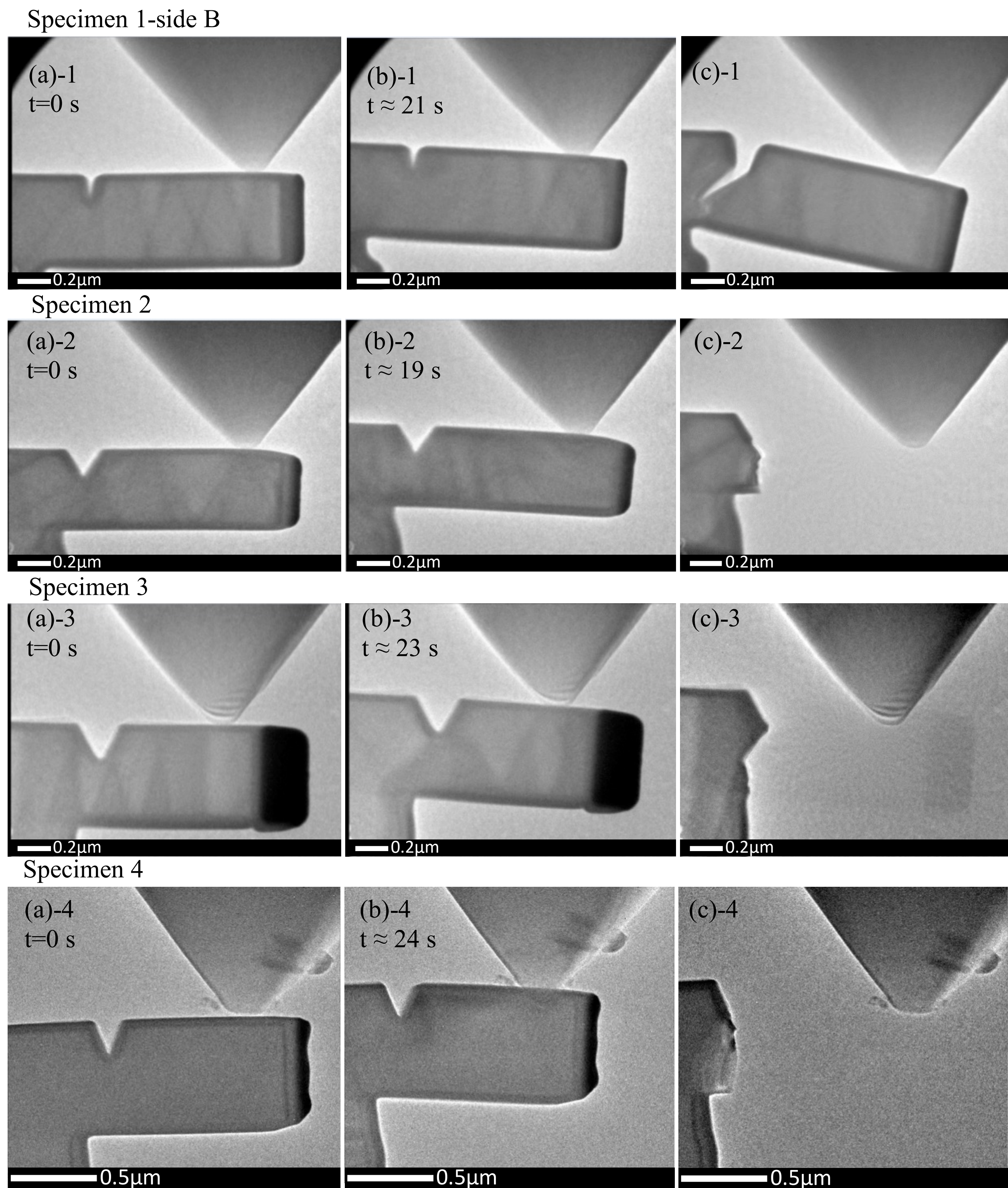

Figure 3. TEM images of the test samples.

The nano-cantilever beams were tested by the procedure outlined in Experimental Section. **Figure 3** shows TEM images of the specimens taken during loading.

The first, second, third and fourth rows represent specimens number 1, 2, 3 and 4, respectively; the first column (i.e., Figure 3(a)1-4) represents the initial instant of the test; the second column (i.e., Figure 3(b)1-4) shows the maximum displacement before final failure;

the last column represents the final failure of the specimens. By re-analyzing the TEM images and videos (see Supporting Information), load-displacement curves were derived for all the nano-cantilever beams and depicted in **Figure 4**. It should be noted that the displacements refer to the end of the cantilever. These curves show the linear relationship between the nominal applied load P and the displacement δ, in accordance with classic beam theory.

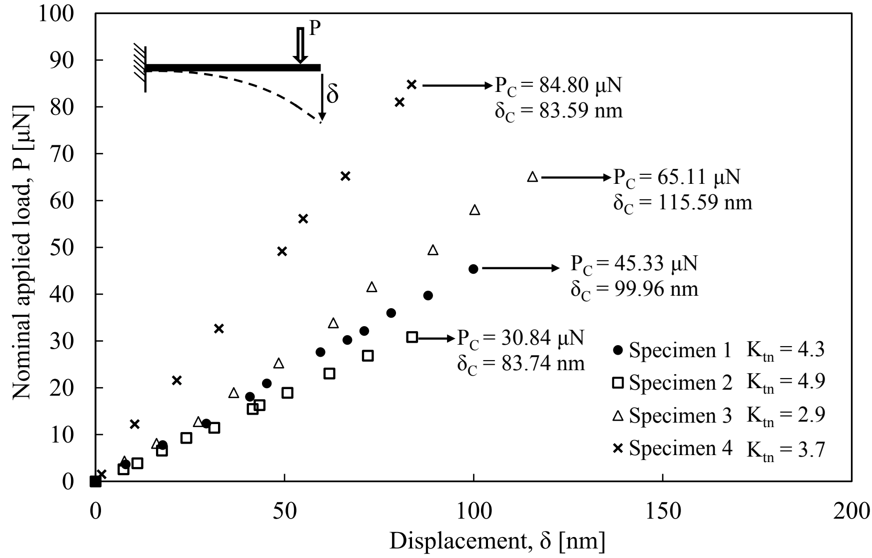

Figure 4. Experimental load-displacement curves.

2.2 Evaluation of the Nano-Si Fracture Toughness by the TCD

Pioneering work on the Theory of Critical Distances (TCD) and "material length parameters" has been conducted by Neuber[29] and Peterson[30] early in the last century, while the recent history of the method has been summarized by Taylor.[31] The TCD can be formalized in different ways, by using, for example, the Point, Line, Area and Volume methods. Considering a notched component under static loading, the Point Method (PM) assumes that "failure occurs when the linear elastic maximum principal stress σ_1 at a given distance r from the notch root equals the inherent material strength of the material σ_0" (see **Figure 5**), that is:[31]

$$\sigma_1\left(\theta = 0, r = \frac{L}{2}\right) = \sigma_0 \tag{1}$$

In the above equation, L is the so-called material characteristic length, which is defined as follows:[32–34]

$$L = \frac{1}{\pi}\left(\frac{K_{IC}}{\sigma_0}\right)^2 \tag{2}$$

Under fatigue-loading, the characteristic material length takes the following form:

$$L = \frac{1}{\pi}\left(\frac{\Delta K_{th}}{\Delta\sigma_0}\right)^2 \quad (3)$$

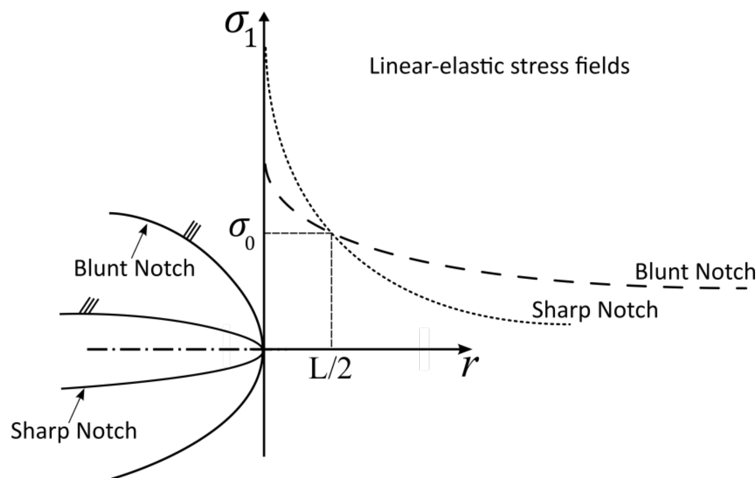

Figure 5. Determination of σ_0 and L to estimate the fracture toughness K_{IC} according to the point method.

The inherent strength σ_0 is a material property and therefore varies depending on the material. However, it has been found that in many brittle and quasi-brittle materials σ_0 is equal to the ultimate tensile stress σ_{UTS}. In general, if plastic deformation occurs before final failure, the inherent strength is found to be different (usually larger) from the expected value. This effect is observed, for example, when polymers are considered.[35] **Equation (1)** and **Equation (2)** indicate that when the material characteristic length and the inherent strength are known, the fracture assessment of a specimen at the nanoscale is performed by analyzing the elastic stress distribution ahead of the notch root, and by comparing the stress value at the distance L/2 with the inherent material strength. On the other hand, the proposed equations can be interpreted differently: if σ_0 ($\Delta\sigma_0$) and L are known *a priori*, the fracture toughness K_{IC} (or ΔK_{th}) can be determined as follows:

$$K_{IC} = \sigma_0\sqrt{\pi L} \quad (4)$$

$$\Delta K_{th} = \Delta\sigma_0\sqrt{\pi L} \quad (5)$$

This attractive strategy seems to fail in the determination of L and of the inherent stress, which, as mentioned above, varies with the material and the amount of plastic deformation involved before final failure. Thus, the approximation $\sigma_0 = \sigma_{UTS}$ may lead to significant errors. To avoid this inconvenience, Susmel et al.[25,36] and Taylor et al.[24,31] proposed an efficient procedure for the determination of TCD parameters based on the assumption that an estimate of fracture toughness as defined in **Equation (4)** can be obtained independently of the notch

geometry considered. More specifically, at least two static tests considering different notch sharpnesses need to be carried out to determine the static strengths. Subsequently, the linear elastic stress fields of the two notches under incipient failure conditions can be plotted and overlapped in a single graph. The intersection of the two linear elastic stress fields then permits the evaluation of both σ_0 and L, as shown in Figure 5 for static cases. Indeed, $L/2$ is the distance between the notch root and the intersection point, along the bisector direction; while σ_0 is the stress at the intersection point. Thus, the fracture toughness can be readily determined by Equation (4). This procedure, in conjunction with Finite Element (FE) analysis, is straightforward and appealing. It has been verified extensively in the references cited, but some precautions must be taken to obtain accurate and reliable results:[25]

- Very different notch geometries should be employed, e.g., sharp and blunt, since this facilitates determination of the intersection point;
- The notch geometries considered must meet the condition $K_t > \frac{\sigma_0}{\sigma_{UTS}}$.

The second point is very critical when blunt geometries are considered: when the notch is too blunt, the stress concentration and weakening effect are lost. In other words, failure may occur when on the net section the stress is close to σ_{UTS}, as happens when plane specimens are considered. It is worth noting that, similar to the procedure summarized here, TCD has also been applied successfully under fatigue,[37,38] mixed-mode loading,[39] elevated temperature,[40] and elastic-plastic conditions.[41]

The evaluation of the fracture toughness by the TCD in the form of the point method (PM) is based on stress analysis ahead of the notch root, as described earlier. Thus, the stress distributions of the principal stress σ_1 referred to the critical load P_C were derived by linear elastic FE analysis summarized in Supporting Information S3. The results are plotted in **Figure 6** on a log-log scale. The beams were subjected to dominant mode I loading and thus the negligible shear stresses are omitted for the sake of brevity and clarity. The intersection between the stress distributions is clear and close to the notch root. The inherent strength σ_0 was 13.9 GPa, while the material characteristic length L varied between 1.3 and 1.9 nm. For these values, the fracture toughness calculated via Equation (4) varied between 0.89 and 1.07 MPa·m$^{0.5}$. The average value was 0.98 MPa·m$^{0.5}$. **Figure 7** compares the fracture toughness values obtained in the present study with the literature values; the scatter is reported when available. The macro-Si K_{IC} is superimposed for the sake of clarity. The average value of 0.98 MPa·m$^{0.5}$ is in good agreement with results obtained by others who fabricated precise pre-

cracks[21,22,26] and is a better estimation than results reported in studies featuring a finite curvature at the crack tip.[19,20]

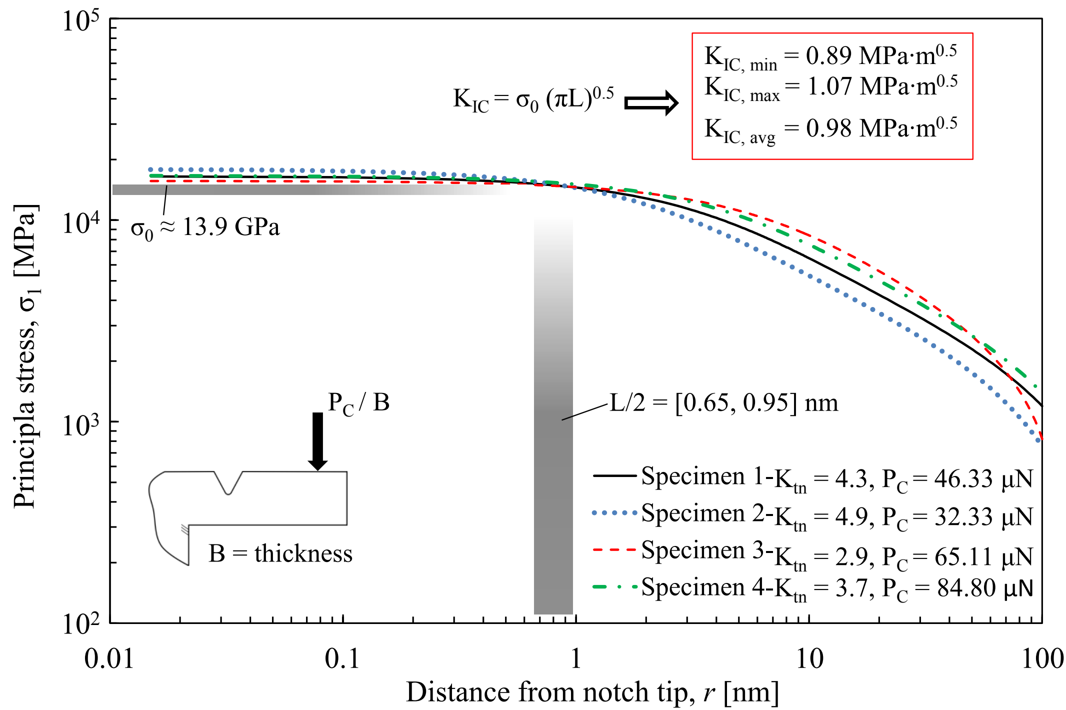

Figure 6. Stress field of the notched nano-cantilever beams and evaluation of K_{IC} in accordance with TCD (point method).

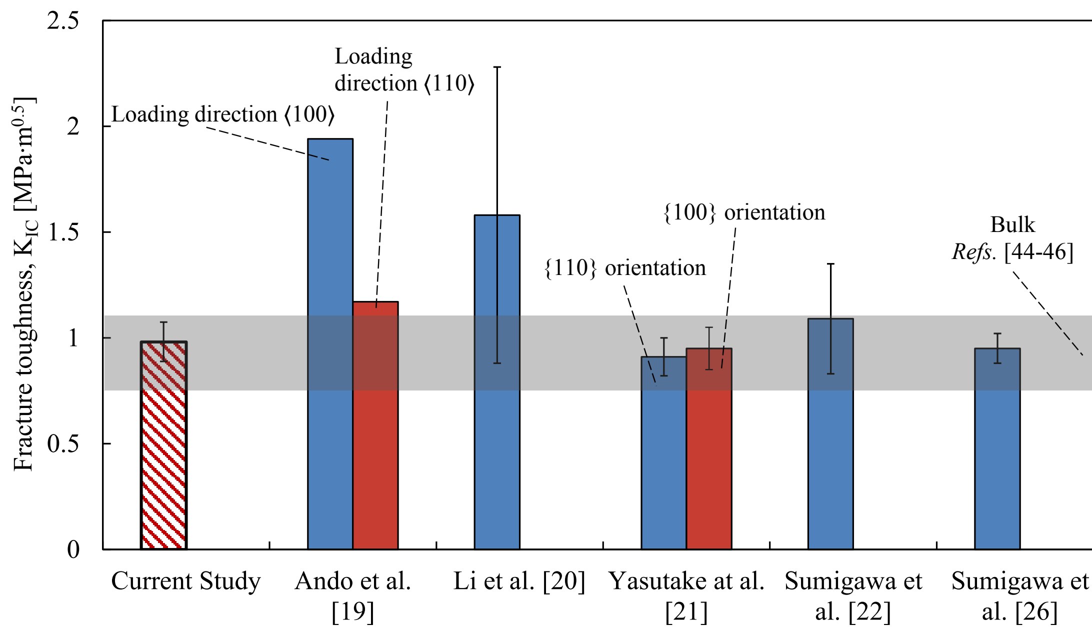

Figure 7. Microscale fracture toughness of single-crystal silicon obtained in the present work and literature values; macro-Si values are superimposed for comparison.

The K_{IC} obtained in the present study by employing just a few samples shows a smaller scatter band in comparison to studies that considered a larger number of specimens. This result confirms that TCD can be used to characterize fracture behavior at very small scales. Also, the fracture toughness is in good agreement with the values reported for the macroscale.[21,23,42–44] This demonstrates that the fracture behavior of silicon is not affected by the size and that micro- nanoscale mechanisms govern the macroscale behavior. On this last point, TCD can yield important findings and further results that are detailed in the Discussion section below.

3. Discussion

The evaluation of the nano-Si K_{IC} is found to be strongly affected by the accuracy in the fabrication of an effective pre-crack. If the crack has a small radius, the fracture toughness is overestimated, and a large scatter is obtained owing to the low reliability in specimen fabrication.[20,45] In some cases, even though a large number of specimens were prepared and tested, the scatter band was still considerable (see Figure 7). Li et al.[20] obtained 3.47 MPa·m$^{0.5}$ in one test which was later excluded during their reanalysis. Figure 6 shows that even when the radius is very small, e.g., only 6.3 nm (specimen 2), the stress distribution does not exhibit the crack singular stress field of $r^{0.5}$. This result proves that small finite curvatures are not tolerated at small scales when conventional methods determine the fracture toughness. Sumigawa et al.[22,26] understood this well and focused on achieving an accurate crack tip. Indeed, their results were in good agreement with the macro-Si fracture toughness and the value obtained in the present study. Thus, accurate control of the final crack geometry, which is currently very challenging, plays an important role in the determination of mechanical fracture properties. The TCD employed here overcomes this problem perfectly, since it does not require any specific restriction on the effective radius achieved: the fracture toughness is determined by comparing the stresses, in incipient failure, of any two sharpnesses of different values. Using TCD, it has been shown experimentally that the K_{IC} obtained in the present study, i.e., 0.98 MPa·m$^{0.5}$, is in perfect agreement with the average K_{IC} for macro-Si and nano-Si values reported in the literature (see Figure 7). All these K_{IC} values have been obtained for different orientations, which demonstrates that the result is independent of the specimen surface orientation. Better yet, the results of the present work showed a smaller scatter than that obtained by others. Better results are obtained only by Sumigawa et al.,[26] who nevertheless needed eight pre-cracked samples. In general, it can be concluded that when

experiments are conducted accurately, the nano-Si K_{IC} and bulk K_{IC} assume the same value, while the tensile strength shows a strong size dependence, as confirmed in the literature.[46–50] This observation suggests that the fracture behavior of silicon is not affected by the size and that the macro- and nano-fracture behavior are governed by the same nanoscale (or even smaller) mechanisms. TCD, in addition to the advantages shown earlier, can correctly yield the magnitude of those small mechanisms.

TCD and some other important concepts of fracture mechanics have only been marginally investigated and considered for application to the micro- and nanoscales. On the other hand, it has been proven that a singular stress field of only several nanometers still governs fracture exactly as it would at the macroscale, but with some limitations due to the breakdown of continuum mechanics.[27] Therefore, the potential of those approaches and in particular of the TCD to be extended to small scales is real. Indeed, TCD lies between the continuum mechanics theories, which assume a homogenous material (e.g., linear elastic fracture mechanics), and the micro-mechanistic approaches that try to model the physical mechanism of the fracture/failure at very small scales. The material characteristic length L can be considered to be a representative length scale parameter that assumes different values as the micro-mechanisms of fracture change scale. Indeed, the determination of L at the microscale/nanoscale allows quantification of the size at which those micro-mechanisms occur. An example is provided by Pugno and Ruoff,[51] who measured the strength of several nanomaterials and showed that the critical distance assumes the size of atomic vacancies; or by Taylor,[52] who demonstrated that L is related to a microstructural length parameter, but this relationship depended on the mechanism involved. The quantity $L/2$ determined in the present study suggests that the mechanism of Si fracture develops at a scale of about 0.65-0.95 nm or, more generally, less than 1 nm. At that small scale, one must deal with the atomic structure. This means: (i) the assumption of continuum mechanics is not valid for smaller scales, i.e., continuum fracture mechanics breaks down, and (ii) the fracture of Si involves the atomic structure, and it may be governed by the cleavage of atomic bonds, i.e., an atomistic interpretation of the brittle fracture of silicon is needed. These statements are reflected in the reanalysis of a recent study by Sumigawa et al.,[26] who analyzed single-crystal Si at the atomic level by density functional theory (DFT) calculations and molecular dynamics (MD) simulations. Sumigawa et al.[26] showed that the initiation of nanocracking was dominated by the cleavage of atomic bonds at the crack tip and found the ideal single-bond strength (regardless of size, geometry, and loading conditions) to be $\sigma_{IS} = 20$ GPa. In addition, they determined the associated fracture toughness by the Griffith criterion (lower bound), $K_{IC,Griffith}$

= 0.77 MPa·m$^{0.5}$, and by DFT simulations (upper bound), $K_{IC,DFT}$ = 1.08 MPa·m$^{0.5}$. Interestingly, the results of the present study, i.e., K_{IC} = 0.89-1.07 MPa·m$^{0.5}$ fall exactly in that range. Recalling now the Irwin formulation, in incipient failure, and re-adapting according to the atomistic interpretation given earlier, i.e.,

$$\sigma_{IS} = \frac{K_{IC}}{\sqrt{\pi a_c}} \tag{6}$$

it is possible to determine a sort of "critical crack length" a_c, equal to 0.47 nm and 0.93 nm on the basis of $K_{IC,Griffith}$ and $K_{IC,\,DFT}$, respectively. Again, it is very interesting to note that the range covered by $L/2$, i.e., 0.65-0.95 nm, falls within these critical crack length values. It is confirmed that TCD correctly suggests a crack propagation in Si governed at the atomic scale and that the range of fracture toughness obtained by re-analyzing the stress distribution of the notched components through TCD correctly predicts the lower and upper bounds reported by Sumigawa et al.[26] In other words, the quantity $L/2$ gives the magnitude of the fracture process, while L may be interpreted as the breakdown of continuum fracture mechanics for singular stress fields approaching that value. This conclusion finds confirmation in the results obtained by Shimada et al.[27], who evaluated the ultimate dimensional limit of fracture mechanics at the nanoscale by considering only several atoms in a singular field near a crack tip. They found that, even though a singular stress field of only several nanometers still governed fracture, stress intensity factors approach failed below a specific singular stress field length. To identify this critical length and hence the breakdown of fracture mechanics, several specimens of different sizes were analyzed. By reducing the plate width, the singular field and the K-dominant field were forced into an ever-shrinking region. On the basis of DFT and molecular dynamics analyses, it was defined a "fracture process zone" Λ_f of 0.4-0.6 nm and a K-dominant region critical size, Λ_k, in the 3-6·Λ_f range, i.e., 1.2-3.6 nm. For values of the singular stress field approaching 1.2-3.6 nm, continuum fracture mechanics breaks down. Interestingly, the TCD proposed in the present study independently yields comparable values: a fracture process zone $L/2$ of 0.65-0.95 nm, slightly higher but comparable to Λ_f; and a material characteristic length L of 1.3-1.9 nm, which is within the range of Λ_k. It is thus demonstrated that the material characteristic length is a representative length scale parameter of the micro-mechanisms of fracture and correctly predicts the breakdown of continuum fracture mechanics in the case of silicon. These results have great impact on the macroscale as well: fracture toughness at the macroscale is governed by the very same mechanisms observed and quantified at the nanoscale, i.e., bond breakage at the atomic level, regardless of the size

and notch shape. Further investigation instead should be carried out considering other materials and scales.

4. Conclusion

The present study used TCD as an alternative methodology for characterizing fracture behavior at the nanoscale. *In situ* micromechanical testing of notched nano-cantilever beams made of single-crystal Si was carried out in a transmission electron microscope. Then, by comparing the stress fields ahead of notches of different sharpnesses, the characteristic material length was determined through TCD.

First, it was shown that the average value of K_{IC} obtained here, i.e., 0.98 $MPam^{0.5}$, was in agreement with the values reported in the literature for the macro- and nanoscale. Thus, the experimental procedure needed for the characterization of fracture behavior was greatly simplified, since the fabrication of an effective crack tip was no longer necessary. Second, TCD yielded the magnitude of the breakdown of fracture mechanics and of the fracture process for Si. These corresponded to the material characteristic length L = 1.3-1.9 nm and $L/2$, respectively. The same range of values has been obtained by other researchers who employed sophisticated DFT and molecular dynamics simulations.[26,27]

It was demonstrated that the fracture toughness of Si is independent of the crystal surface orientation and of the scale considered: from the macroscale to the nanoscale, the mechanism governing fracture involves the cleavage of atomic bonds.

The present study puts forth a new methodology for the characterization of fracture properties at the micro- and nanoscales. Indeed, the TCD can be applied to a large variety of materials, such as composites materials, polymers, ceramics and even biomaterials (e.g., bones). It provides a tool for the evaluation of the fracture mechanics properties by characterizing the breakdown of continuum fracture mechanics. The consideration of smaller scales is left for future work. Some preliminary results have been obtained by Shimada et al.,[26] who proposed a general method to account for non-continuum conditions by extending the Griffith criterion beyond its scale limit.

5. Experimental Section

Material and Specimen Fabrication: Single-crystal silicon is an anisotropic material with cubic symmetry that shows brittle behavior up to final failure (at room temperature). Its mechanical properties depend on the crystal orientation, but it is a particular linear elastic orthotropic material. Thus, its constitutive law is very simple and can be parameterized by the

three material constants C_{11} = 167.4 GPa, C_{22} = 65.23 GPa and C_{44} = 79.57 GPa. Alternatively to these three constants, Young's modulus for each direction can be determined by a combination of C_{11}, C_{22}, and C_{44}, in accordance with the stiffness matrix.[53] This alternative procedure is particularly useful when in-plane loads and 2D models are considered since the material can be simplified and treated as being isotropic. The specimens made of single-crystal Si were prepared by a focused ion beam (FIB) processing system (Hitachi High-Tech FB-2100FIB). During FIB fabrication, the accelerating voltage was 40 kV, and the beam currents for rough and fine processing were 1.13 nA and 0.01 nA, respectively. Detailed fabrication steps are reported in the Supporting Information (see section S1). The sharpness of the notch was governed by the FIB processing time: sharp (blunt) notches are obtained by short (long) processing times. Although there is a protective layer on the front surface of the block, a damaged layer (< 10 nm thick) is formed on the other surfaces while cutting the nano-cantilever. However, the effect of this damaged layer is negligible since it is very small compared to the final thickness and length of the specimens.

In-situ Micromechanical Testing: The loading experiments are conducted under vacuum in a Transmission Electron Microscope (TEM) using a sample holder with a loading device (Nanofactory Instruments AB, SA2000N). The TEM is equipped with an *in situ* camera (Gatan, ES500). The loading device consists of a stage that can be freely moved in the space to adjust its position and has a diamond loading tip. The stage is driven by a piezoelectric actuator with a displacement accuracy of approximately 1 nm. The load is applied to the specimens by being pushed onto the wedge-shaped diamond indenter. The applied load is detected by a load sensor beneath the indenter (measurement range: 0-1000 μN, resolution of loading: 0.1 μN). Photographs of the micromechanical testing system are given in **Figure S2** (see Supporting Information). The loading process up to final failure is recorded by the *in situ* camera, and the deflection of the nano-cantilever δ is obtained by analyzing the TEM images. The geometry of the specimens is analyzed by SEM, while the deflection by TEM and the two microscopes may have a different scale. For this reason, the deflection as recorded by the TEM is scaled to match the measurements of the SEM. Particularly, TEM deflections observed for the specimen 1, 2, 3 and 4 are scaled down by a factor 1.13, 1.08, 1.18 and 1.26, respectively. These factors are obtained by the ratio of the specimens height W given by the TEM and SEM, respectively.

Supporting Information

Supporting Information is available from the Wiley Online Library or from the author.

Acknowledgements

This work was supported by the Japan Society for the Promotion of Science (JSPS), International Research Fellow program Grant Number 16F16366; JSPS KAKENHI Grant Number JP15H02210, JP26630009 and JP25000012. P. Gallo wrote the paper, planned and supervised experiments, reanalyzed the results; Y. Yan carried out the experiments; T. Sumigawa and T. Kitamura discussed the results, gave valuable comments on the entire study and reviewed the manuscript.

Received: ((will be filled in by the editorial staff))
Revised: ((will be filled in by the editorial staff))
Published online: ((will be filled in by the editorial staff))

References

[1] H. Ohnishi, Y. Kondo, K. Takayanagi, *Nature* **1998**, *395*, 780.
[2] V. Rodrigues, D. Ugarte, *Phys. Rev. B* **2001**, *63*, 73405.
[3] R. H. Baughman, *Science (80-.).* **2002**, *297*, 787.
[4] T. Kitamura, T. Sumigawa, H. Hirakata, T. Shimada, *Fracture Nanomechanics*, Pan Stanford Publishing, **2016**.
[5] W. N. Sharpe, B. Yuan, R. L. Edwards, *J. Microelectromechanical Syst.* **1997**, *6*, 193.
[6] K. Sato, T. Yoshioka, T. Ando, M. Shikida, T. Kawabata, *Sensors Actuators A Phys.* **1998**, *70*, 148.
[7] T. Yi, L. Li, C. J. Kim, *Sensors Actuators A Phys.* **2000**, *83*, 172.
[8] F. Ericson, J. Schweitz, *J. Appl. Phys.* **1990**, *68*, 5840.
[9] A. Bower, *Applied Mechanics of Solids*, CRC Press, **2009**.
[10] T. Sumigawa, H. Fang, E. Kawai, T. Kitamura, *Mech. Eng. Rev.* **2014**, *1*, SMM0007.
[11] S. W. Cho, I. Chasiotis, *Exp. Mech.* **2007**, *47*, 37.
[12] M. A. Haque, M. T. A. Saif, *Exp. Mech.* **2003**, *43*, 248.
[13] T. Sumigawa, T. Kitamura, in *Transm. Electron Microsc.* (Ed: K. Maaz), InTech, **2012**, pp. 355–380.
[14] P. Gallo, T. Sumigawa, T. Kitamura, F. Berto, *Fatigue Fract. Eng. Mater. Struct.* **2016**,

39, 1557.

[15] F. Berto, P. Lazzarin, *Theor. Appl. Fract. Mech.* **2009**, *52*, 183.

[16] F. Berto, P. Lazzarin, *Mater. Sci. Eng. R Reports* **2014**, *75*, 1.

[17] A. Masolin, P. O. Bouchard, R. Martini, M. Bernacki, *J. Mater. Sci.* **2013**, *48*, 979.

[18] B. N. Jaya, J. M. Wheeler, J. Wehrs, J. P. Best, R. Soler, J. Michler, C. Kirchlechner, G. Dehm, *Nano Lett.* **2016**, *16*, 7597.

[19] T. Ando, X. Li, S. Nakao, T. Kasai, H. Tanaka, M. Shikida, K. Sato, *Fatigue Fract. Eng. Mater. Struct.* **2005**, *28*, 687.

[20] X. Li, T. Kasai, S. Nakao, H. Tanaka, T. Ando, M. Shikida, K. Sato, *Sensors Actuators, A Phys.* **2005**, *119*, 229.

[21] K. Yasutake, M. Iwata, K. Yoshii, M. Umeno, H. Kawabe, *J. Mater. Sci.* **1986**, *21*, 2185.

[22] T. Sumigawa, S. Ashida, S. Tanaka, K. Sanada, T. Kitamura, *Eng. Fract. Mech.* **2015**, *150*, 161.

[23] M. Tanaka, K. Higashida, H. Nakashima, H. Takagi, M. Fujiwara, *Mater. Trans.* **2003**, *44*, 681.

[24] D. Taylor, *The Theory of Critical Distances: A New Perspective in Fracture Mechanics*, Oxfor, **2007**.

[25] L. Susmel, D. Taylor, *Eng. Fract. Mech.* **2010**, *77*, 1492.

[26] T. Sumigawa, T. Shimada, S. Tanaka, H. Unno, N. Ozaki, S. Ashida, T. Kitamura, *ACS Nano* **2017**, acsnano.7b02493.

[27] T. Shimada, K. Ouchi, Y. Chihara, T. Kitamura, *Sci. Rep.* **2015**, *5*, 8596.

[28] J. Schindelin, I. Arganda-Carreras, E. Frise, V. Kaynig, M. Longair, T. Pietzsch, S. Preibisch, C. Rueden, S. Saalfeld, B. Schmid, J.-Y. Tinevez, D. J. White, V. Hartenstein, K. Eliceiri, P. Tomancak, A. Cardona, *Nat. Methods* **2012**, *9*, 676.

[29] H. Neuber, *Theory of Notch Stresses: Principles for Exact Calculation of Strength with Reference to Structural Form and Material*, Springer-Verlag, Berlin, **1958**.

[30] R. E. Peterson, in *Met. Fatigue* (Eds: G. Sines, J.L. Waisman), McGraw-Hill, New Yorl, **1959**, pp. 293–306.

[31] D. Taylor, *Eng. Fract. Mech.* **2008**, *75*, 1696.

[32] K. Tanaka, *Int. J. Fract.* **1983**, *22*, 39.

[33] D. Taylor, *Int. J. Fatigue* **1999**, *21*, 413.

[34] M. H. El Haddad, K. N. Smith, T. H. Topper, *J. Eng. Mater. Technol.* **1979**, *101*, 42.

[35] D. Taylor, M. Merlo, R. Pegley, M. P. Cavatorta, *Mater. Sci. Eng. A* **2004**, *382*, 288.

[36] L. Susmel, D. Taylor, *Eng. Fract. Mech.* **2008**, *75*, 4410.

[37] L. Susmel, *Eng. Fract. Mech.* **2008**, *75*, 1706.

[38] J. A. Araújo, L. Susmel, M. S. T. Pires, F. C. Castro, *Tribol. Int.* **2017**, *108*, 2.

[39] L. Susmel, D. Taylor, *Eng. Fract. Mech.* **2008**, *75*, 534.

[40] R. Louks, L. Susmel, *Fatigue Fract. Eng. Mater. Struct.* **2015**, *38*, 629.

[41] L. Susmel, D. Taylor, *J. Eng. Mater. Technol.* **2010**, *132*, 21002.

[42] R. D. Dukino, M. V. Swain, *J. Am. Ceram. Soc.* **1992**, *75*, 3299.

[43] C. P. Chen, M. H. Leipold, *Am. Ceram. Soc. Bull.* **1980**, *59*, 469.

[44] B. Wong, *J. Electrochem. Soc.* **1987**, *134*, 2254.

[45] T. Ando, M. Shikida, K. Sato, *Sensors Actuators, A Phys.* **2001**, *93*, 70.

[46] G. Stan, S. Krylyuk, A. V. Davydov, R. F. Cook, *J. Mater. Res.* **2011**, *27*, 562.

[47] M. R. He, J. Zhu, *Phys. Rev. B - Condens. Matter Mater. Phys.* **2011**, *83*, 1.

[48] S. Sundararajan, B. Bhushan, *Sensors Actuators, A Phys.* **2002**, *101*, 338.

[49] S. Hoffmann, F. Östlund, J. Michler, H. J. Fan, M. Zacharias, S. H. Christiansen, C. Ballif, *Nanotechnology* **2007**, *18*, 205503.

[50] B. Moser, K. Wasmer, L. Barbieri, J. Michler, *J. Mater. Res.* **2007**, *22*, 1004.

[51] N. M. Pugno, R. S. Ruoff, *Philos. Mag.* **2004**, *84*, 2829.

[52] D. Taylor, *Theor. Appl. Fract. Mech.* **2017**, *90*, 228.

[53] J. J. Wortman, R. A. Evans, *J. Appl. Phys.* **1965**, *36*, 153.